Enhancement of energetic electrons and protons by cone guiding of laser light

Z. L. Chen,* R. Kodama, M. Nakatsutsumi, H. Nakamura, M. Tampo, K. A. Tanaka, Y. Toyama, T. Tsutsumi, and T. Yabuuchi
Institute of Laser Engineering, Osaka University, 2-6 Yamada-oka, Suita, Osaka 565-0871, Japan
(Received 27 February 2004; revised manuscript received 26 July 2004; published 16 March 2005)

Energetic electrons and protons are observed when a target consisting of a reentrant cone with a disk at the tip is irradiated by a petawatt (PW) laser at an intensity of approximately 10^{19} W cm^{-2}. The angular distribution of the electrons and protons, dependent on the open angle of the reentrant cone, is found to differ from that in the case when a target with planar geometry is used. Two jet beams are observed, in directions parallel to the cone axis and normal to the cone-shaped wall. The number and cutoff energies of the generated protons are also related to the open angle of the cone. The efficiency of the generation of energetic electrons from the cone target is 2-3 times higher than that from a simple plane target. These results indicate a guiding of the PW laser beam in the cone geometry.

DOI: 10.1103/PhysRevE.71.036403 PACS number(s): 52.38.−r, 52.75.−d, 41.75.−i

In order to achieve laser fusion with high gain, the thermonuclear fuel must be at extremely high densities and temperatures [1]. A fuel with very high density of up to 1000 times greater than the solid has thus far been achieved [2]. Sufficiently high temperatures can be attained using the base-line central hot-spot approach, which uses shock waves to heat a small volume of the dense core of the compressed fuel pellets [1]. Alternatively, the technique of "fast ignition" has the potential to ignite the dense core by using a very intense laser pulse [3]. However, the realization of this concept is challenging since the core is hidden under a plasma corona with a long scale length, which is opaque to the laser pulse. To overcome this problem, one must use the laser beam to efficiently create a beam of charged particles that deposit their energy in a localized volume of the assembled core. In preliminary studies a laser prepulse was used to clear a path deep into the plasma, allowing the subsequent ignition pulse to penetrate close to the core to create a spray of electrons [4]. Previous experiments have demonstrated an efficient production of electrons [5] and the occurrence of tunnel digging [6], but it appears to be difficult to extend the digging to get sufficiently close to a very dense core. The plasma surrounding the compressed core in the center of the pellet can give rise to large energy losses by deflecting the ultraintense laser pulse, severely decreasing the efficiency of the coupling between the laser and the dense core. An alternative to laser prepulse techniques is the use of a reentrant cone to block the formation of a plasma atmosphere in front of the core. This allows the ignition laser a clear path and close approach to the assembled core and a well-defined surface at which to create electrons [7]. The increase in neutron yield obtained by using this cone target with a 0.5-PW laser confirms that a higher coupling efficiency between the laser and pellet is achieved [8].

The details of the interaction between the laser and reentrant cone and the precise mechanism responsible for this enhanced coupling efficiency between the laser and compressed fuel are presently unclear. Understanding this process is critically important in assessing the feasibility of scaling cone targets to full fast ignition conditions. Simulations using cone geometry predict that microfocusing of the laser beam will occur, resulting in enhanced electron generation [9]. However, it is also essential to perform experiments in order to understand the physics of cone targets in detail.

In this paper, we report experimental studies of the interaction of a PW laser beam with a cone geometry target. We have investigated the generation of energetic electrons and protons, including their angular distribution, for open cone angles of 30° and 60°. The angular distribution pattern was completely different to that obtained from a simple planar target; two jet beams, one close to the cone axis and the other normal to the cone wall, were observed both for protons and electrons. The number of electrons generated using the cone geometry was greatly enhanced in comparison to the simple planar target. The generation of protons and their cutoff energy were found to depend on the exact geometry of the cone target. Our data can be explained by the way in which laser light is guided in cone geometry.

Experiments were performed using the PW beam [10] of the Gekko XII laser facility at the Institute of Laser Engineering at Osaka University. A 0.75-ps laser pulse with a wavelength of 1.06 μm and an energy of 180 J was focused, with 40% of the energy concentrated into a 20×50 μm^2 diameter elliptical spot, by an off-axis parabola mirror ($f/7$). A peak intensity of approximately 1×10^{19} W cm^{-2} was obtained at the target.

Two types of reentrant cone targets were used, with open angles of 30° and 60°. The targets consisted of a gold cone wall with a gold disk at the tip and are shown in Fig. 1. The inner diameter of the disk was approximately 30–45 μm and it was 7 μm thick. The wall was approximately 20 μm thick and 900 μm long. The incident laser beam was directed normal to the disk, along the cone axis.

A sandwichlike detector was used to observe the angular distribution of the generated electrons and protons at different energies in the forward laser direction. This detector consisted of multiple layers of radiochromic films (RCF's), CR-39's (see below), and imaging plates (IP's), arranged

*Electronic address: chen@ile.osaka-u.ac.jp; zhenglinchen@hotmail.com

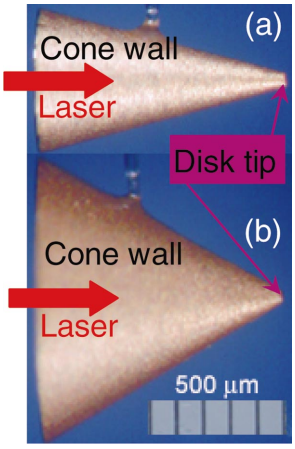

FIG. 1. (Color) Cone targets with open angles of (a) 30° and (b) 60°. The targets consisted of a gold reentrant cone wall with a gold disk at the tip. The disk was approximately 30–45 μm in inner diameter and 7 μm thick. The cone-shaped wall was approximately 20 μm thick and 900 μm long. The laser beam was incident in a direction normal to the disk, along the cone axis.

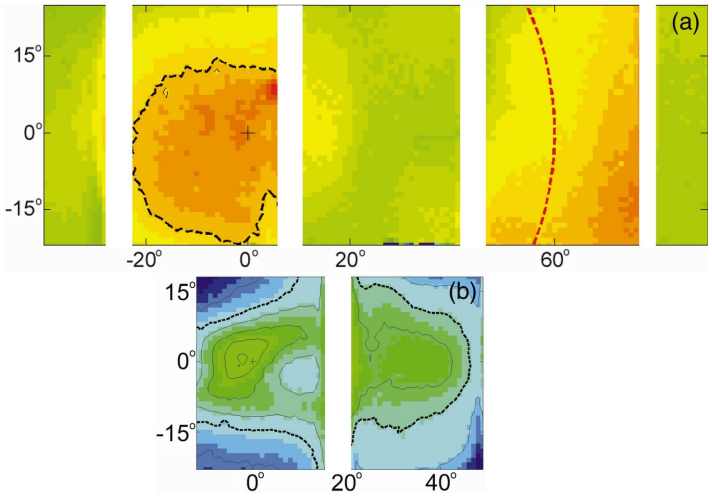

FIG. 2. (Color) Angular distributions of electrons with energies of over 1.3 MeV from (a) a 60° cone target and (b) a plane target with an incident angle of 60°, measured by the IP in the forward laser direction with the laser horizontally polarized. The color scale indicates the number of electrons, with red representing greater numbers. The black dotted lines show the full angular width of the electron jet at half of the maximum electron number. Crosses in both images show the laser beam direction (0 degrees on both axes). The red dotted line in (a) depicts the wall normal.

periodically. The relevant energy ranges, 1.3–11.3 MeV for electrons and 0.7–21.8 MeV for protons, were selected using plastic filters and copper foils inserted into the detector. The detector was enclosed by Al foils and black tapes in order to block scattered light. A 10-μm-thick Al foil was placed at the front of the detector to shield it from the target debris; this foil is able to stop nearly all of the heavy ions. CR-39 is a plastic nuclear track detector, sensitive only to ions with energies of greater than 100 keV/nucleon [11,12]. Ion images can be obtained by etching the CR-39 in sodium hydroxide under appropriate conditions. RCF's consist of a transparent material (typically nylon) coated with an organic dye [11,12]. Upon exposure to ionizing radiation the film undergoes a color change. The optical density of the film is then measured, enabling the total number of energetic protons passing through the film at each point to be determined. RCF's can also detect electrons, ions, or hard x rays, with different sensitivities. One can determine whether the radiation detected by an RCF corresponds to ions by comparing the image to that on the CR-39. The IP is a two-dimensional radiation sensor that utilizes photon-stimulated luminescence (PSL) in $BaFBr:Eu^{3+}$ [13]. It is sensitive to all radiation including scattered light, electrons, x rays, and ions. The scattered light, energetic ions, and protons were completely shielded in our experiments so that only the energetic electrons and hard x rays were detected by the IP's.

The angular distribution of electrons with energies over 1.3 MeV escaping from both a 60° cone target and a plane target in the forward laser direction is shown in Fig. 2. Two jets of electrons were emitted from the cone target, one along the cone axis and the other normal to the cone wall (the latter was not observed when the 30° cone was used). The divergence of the jet parallel to the incident laser beam is less than 30° for the cone target, whereas it is over 40° for the plane target irradiated by a horizontally polarized laser incident at 60° to the target normal. The larger divergence of electrons from the plane target is attributed to the lower effective laser intensity that results from the open geometry and the large incident angle of 60°. A combination of absorption mechanisms including $\vec{J}\times\vec{B}$ [14] and Brunel absorption [15] might also increase the divergence when the incident laser beam is at oblique angle to the target; these mechanisms accelerate electrons in directions both parallel to the laser axis and normal to the target [16].

The electron energy spectra measured in the forward laser direction from all three types of targets are compared in Fig. 3. These spectra are derived from the angular distribution measurement described above; four layers of the IP and three layers of the copper filter in the sandwichlike detector allow electrons to be selected at four different energy levels. It was observed that 2-3 times more electrons were emitted from the cone targets than from the plane target. This indicates that cone geometry improves the coupling between the laser and target, resulting in a more efficient energy transfer from the laser to the electrons. Furthermore, the number of electrons at high energies (here larger than 4 MeV) emitted from the 30° cone was greater than that from the 60° cone, although there was no difference in the number of electrons at low energies (here approximately 1.5 MeV). This implies that the energy transfer from the laser to the electrons is better for the 30° cone than for the 60° cone.

The angular distribution of protons in the energy range 0.7–5 MeV emitted from cone targets with open angles of 60° and 30° and measured by RCF is shown in Fig. 4. In similar fashion to the electrons in Fig. 2(a), two proton beams close to the cone axis and normal to the cone wall were observed in the forward laser direction. The beam parallel to the 30° cone axis was much more intense than that in the 60° cone; the latter beam could only be detected by the CR-39 since its intensity was too weak to be clearly seen

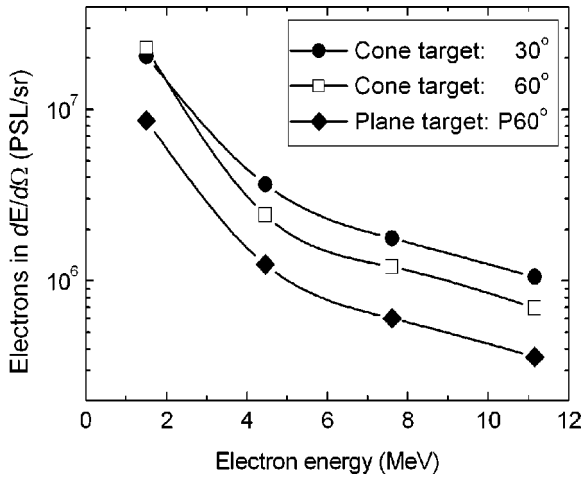

FIG. 3. Energetic electron spectra in the forward laser direction obtained from gold cone targets with open angles of 30° (circles) and 60° (rectangles) and from a plane target with an incident angle of 60° (diamonds), estimated from IP data showing angular distributions such as those in Fig. 2.

using the RCF's. The intensity of the proton beam normal to the cone wall was similar in both cases.

Further comparisons between the different target geometries are summarized in Table I. The emission of light from the rear surface of an Al foil positioned at the tip of the 60° reentrant cone is 2–3 times stronger than that from the simple planar Al target, indicating an increased heating of the foil by energetic electrons when a cone target is used [17]. Cone targets also give rise to an increase in the proton

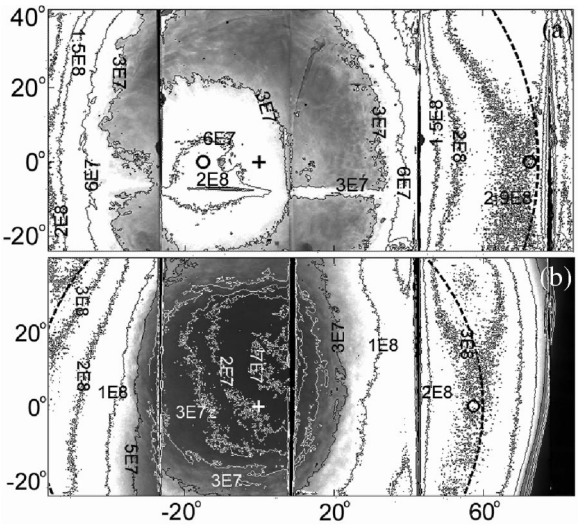

FIG. 4. Angular distributions of protons at energies of 0.7–5 MeV in the forward laser direction from the cone targets with open angles of (a) 30° and (b) 60°, with the laser horizontally polarized, measured using RCF's. The gray scale indicates the number of protons, with the brighter regions representing larger numbers. The solid lines are proton number contours, where the numerical values show the deposited energies in MeV per solid angle. Dotted lines show the normal to the cone-shaped wall. The circles and crosses correspond to the local peak proton count and to the laser beam direction (0° on both axes), respectively.

cutoff energy, which was found to be 10 MeV for the plane target, 12 MeV for the 60° cone, and 15 MeV for the 30° cone.

The improvement in energy transfer from the laser to the electrons in the cone targets can be explained by the way in which the cone geometry guides laser light. In our experiments, 40% of the laser energy is focused in the $20 \times 50\ \mu m^2$ spot, whereas the disk at the tip of the cone targets is 30–45 μm in diameter. This implies that approximately 60% of the laser energy is situated outside the disk and hence interacts with the wall. The contrast ratio of the laser prepulse to the main pulse (less than 10^{-8}) ensures that the cone geometry is successfully preserved for the 0.75 ps duration of the interaction (the length of the laser pulse). The laser beam incident upon the wall would thus be absorbed via processes induced by the electric field such as Brunel [15] or resonance [18] absorption, and also absorbed via the $\vec{J}\times\vec{B}$ mechanism [14]. In addition, it would be reflected in the specular direction. After being absorbed and reflected by the wall several times, the laser beam is guided to a tiny spot at the disk, enhancing the effective laser intensity as well as the absorbed energy at the disk, as predicted by particle-in-cell simulations [9]. It is expected that this process would increase the number of electrons generated, as shown in Figs. 2 and 3 and Table I. Enhancement of the laser intensity at the disk would also play an important role in decreasing the divergence of the electron beam parallel to the laser axis in comparison with the plane target, as demonstrated in Fig. 2 and Table I.

In order to quantify the energy of the laser light incident at the disk in the cone geometry, we used simple ray-tracing techniques to calculate values for the 30° and 60° cones and compare them with the plane geometry. In this calculation, the laser beam was focused on a 30-μm disk through an $f/7$ optic to produce a Gaussian shape with a diameter of 30 μm [full width at half maximum (FWHM)]. Absorption at the wall was assumed to be 20% for the *s*-polarized beam and for incident light normal to the wall, but it varies with different incidence angles, corresponding to the angular dependence of Brunel absorption [15], in the case of *p* polarization. The results of the calculations showed that the concentration of energy at the disk is enhanced by a factor of 1.5 in the 60° cone and by 2 in the 30° cone, relative to the plane target. This is consistent with our experimental results — the cone disk was observed to collect a larger amount of laser energy due to side wall reflection. The absorption rate and reflection times from the side wall of the 60° cone are larger than those for the 30° cone due to the incident angle dependence of Brunel absorption and the optical geometry. Therefore, more efficient guiding of the laser light to the disk can be expected for the 30° cone, which is consistent with the experimental results as seen in the electron energy spectra in Fig. 3 and the proton angular distributions in Fig. 4.

The guiding of laser light in the cone can also explain the distribution patterns of the MeV electrons and protons. The jet parallel to the cone axis mainly results from $\vec{J}\times\vec{B}$ absorption of directly interacting light and light reflected from the side wall. The jet normal to the rear cone-shaped wall must

TABLE I. Comparison of MeV protons and electrons generated from cone targets with open angles of 30° and 60° and from the plane target with an incident angle of 60°. The results of rear emission induced by electron heating were given in Ref. [17]. Here we normalized rear emission and the number of electrons in the plane target to 1.

	Plane	60° cone	30° cone
Proton cutoff energy	$<$10 MeV	$<$12 MeV	$<$15 MeV
Rear emission due to electrons [17]	1	2–3	⋯
Electron divergence angle	$\geqslant$about 30°–40°	$\leqslant$about 30°	$\leqslant$about 30°
Electron number in forward laser direction	1	2–3	$>$2–3

arise from absorption of the oblique beam at the side wall via the electric field, through a process such as Brunel absorption. The dependence of the results on the cone angle indicates a difference in the guiding of laser light in the two cones. More laser light would be reflected from the side wall to the tip of the 30° cone than for the 60° cone, taking into account the incident angle dependence of Brunel absorption [15].

The more efficient guiding of laser light into the disk at the tip in the 30° cone relative to the 60° cone is also consistent with the increased degree of proton generation along the cone axis, as shown in Fig. 4, and the higher-energy cutoff for the protons, as shown in Table I. MeV protons are usually generated in ultraintense laser interactions and accelerated in a direction normal to the rear of the target by a sheathlike potential [12]. The proton beam parallel to the cone axis is thus related to the effective laser intensity at the disk. In the 30° cone geometry, more laser energy is guided to the disk by the wall and the laser intensity at the disk is therefore higher than that for the 60° cone. More energetic electrons are thus produced, which then propagate to the rear surface of the disk, inducing a more intense sheathlike potential for the 30° cone. Consequently, it is possible to generate more MeV protons, which also have a higher cutoff energy, along the axis of the 30° cone. The scaling law for the dependence of the proton cutoff energy upon laser intensity [19], which is $E_{max} \propto I^{0.3-0.5}$, suggests that the laser intensity at the disk for the 30° cone target could be enhanced by a factor of 3 relative to that in the plane geometry. This enhancement may be consistent with predictions given by simple ray-tracing calculations. All the data indicate that more laser energy is guided by the side wall to the disk at the tip of the 30° cone than to the tip of the 60° cone.

In addition to guiding laser beams, the cone geometry is also expected to guide electrons due to the presence of spontaneous magnetic and electric fields surrounding the cone [9,17], resulting in an enhancement of the electron beam from the disk. The observation of a proton beam close to the normal of the cone-shaped wall, with the precise direction of the beam dependent upon its energy (for example, 10-MeV protons are deflected by 10°–15°), indicates the existence of a MG magnetic field. This self-generated magnetic field, together with an electric field such as the sheathlike potential, might confine the electrons and guide them along the wall to the tip of the cone; details of these fields and their effects will be the subject of future studies.

In conclusion, we have investigated MeV electron and proton generation from targets with cone geometry using a PW laser. The number of MeV electrons parallel to the cone axis is increased by a factor of 2–3 in the cone geometry relative to the open plane geometry. The effect of the cone angle on the generation of electrons and protons was also investigated, using 30° and 60° cones. Much brighter emission and higher cutoff energies are observed for protons along the axis of the 30° cone compared to the 60° cone. All of these results are explained by the way in which laser light is guided in the cone geometry. The cone-shaped wall acts like a "plasma mirror" to guide scattered laser light to the tip of the cone, resulting in higher laser intensity at the disk at the cone tip. This guiding effect is more pronounced when the cone with the smaller open angle is used. Enhancements in the laser intensity and in the generation of energetic electrons and protons ought to depend on the detailed geometry of the target and on the laser characteristics. These results, in combination with more detailed studies, will allow cone target geometry to be optimized in order to efficiently guide the laser beam. Therefore, control of laser intensity and laser absorption at the tip of the cone will be possible in the future.

The authors would like to thank the technical staff at the Institute of Laser Engineering for their support with the operation of the laser system, target fabrication, and data acquisition. Special thanks are due to Dr. R. A. Snavely (in Lawrence Livermore National Laboratory, USA) for his kind help with the proton detector and to Dr. G. R. Kumar (in Tata Institute of Fundamental Research, India) for fruitful discussions.

[1] J. Lindl, Phys. Plasmas **12**, 3933 (1995).

[2] H. Azechi *et al.*, Laser Part. Beams **9**, 193 (1991).

[3] N. G. Basov *et al.*, J. Sov. Laser Res. **13**, 396 (1992); M. Tabak *et al.*, Phys. Plasmas **1**, 1626 (1994).

[4] A. Pukhov and J. Meyer-ter-Vehn, Phys. Rev. Lett. **79**, 2686 (1997).

[5] M. Tatarakis *et al.*, Phys. Rev. Lett. **81**, 999 (1998); L. Gremillet *et al.*, *ibid.* **83**, 5015 (1999); M. Borghesi *et al.*, *ibid.* **83**,

4309 (1999); H. Ruhl *et al.*, *ibid.* **82**, 743 (1999); W. Yu *et al.*, *ibid.* **85**, 570 (2000); R. Kodama *et al.*, *ibid.* **84**, 674 (2000); M. I. K. Santala *et al.*, *ibid.* **84**, 1459 (2000); X. F. Wang *et al.*, *ibid.* **84**, 5324 (2000); M. I. K. Santala *et al.*, *ibid.* **86**, 1227 (2001).

[6] P. E. Young *et al.*, Phys. Rev. Lett. **63**, 2812 (1989); P. Sprange, E. Esary, and A. Ting, *ibid.* **64**, 2011 (1990); P. Sprange *et al.*, *ibid.* **69**, 15 (1992); S. C. Wilks *et al.*, *ibid.* **69**, 1383 (1992); P. E. Young *et al.*, *ibid.* **75**, 1082 (1995); P. E. Young *et al.*, Phys. Plasmas **2**, 2825 (1995); C. A. Coverdale *et al.*, Phys. Rev. Lett. **74**, 4659 (1995); R. Kodama *et al.*, *ibid.* **77**, 4906 (1996); A. Pukhov and J. Meyer-ter-Vehn, *ibid.* **76**, 3975 (1996); M. Zepf *et al.*, Phys. Plasmas **3**, 3242 (1996); P. Gibbon and E. Forster, Plasma Phys. Controlled Fusion **38**, 769 (1996); M. Borghesi *et al.*, Phys. Rev. Lett. **78**, 879 (1997); R. Wanger *et al.*, *ibid.* **78**, 3125 (1997); K. Krushelnick *et al.*, *ibid.* **78**, 4047 (1997); V. Malka *et al.*, *ibid.* **79**, 2979 (1997).

[7] P. A. Norreys *et al.*, Phys. Plasmas **7**, 3721 (2000).

[8] R. Kodama *et al.*, Nature (London) **412**, 798 (2001); M. H. Key, *ibid.* **412**, 775 (2001); R. Kodama *et al.*, *ibid.* **418**, 933 (2002).

[9] Y. Sentoku *et al.*, Phys. Plasmas **11**, 3083 (2004).

[10] Y. Kitagawa *et al.*, IEEE J. Quantum Electron. **40**, 281 (2004).

[11] E. L. Clark *et al.*, Phys. Rev. Lett. **84**, 670 (2000); A. Maksimchuk *et al.*, *ibid.* **84**, 4108 (2000); E. L. Clark *et al.*, *ibid.* **85**, 1654 (2000).

[12] S. P. Hatchett *et al.*, Phys. Plasmas **7**, 2076 (2000); R. Snavely *et al.*, Phys. Rev. Lett. **85**, 2945 (2000); S. C. Wilks *et al.*, Phys. Plasmas **8**, 542 (2001); A. J. Mackinnon *et al.*, Phys. Rev. Lett. **86**, 1769 (2001); A. J. Mackinnon *et al.*, *ibid.* **88**, 215006 (2002); M. Hegelich *et al.*, *ibid.* **89**, 085002 (2002).

[13] T. Takahashi *et al.*, Ionizing Radiation **28**, 203 (2002) (in Japanese).

[14] P. J. Catto and R. M. More, Phys. Fluids **20**, 704 (1977); W. L. Kruer and K. Estabrook, *ibid.* **28**, 430 (1985); T.-Y. B. Yang *et al.*, Phys. Plasmas **2**, 3146 (1995); W. Rozmus *et al.*, *ibid.* **3**, 360 (1996); T.-Y. B. Yang *et al.*, *ibid.* **3**, 2702 (1996).

[15] F. Brunel, Phys. Rev. Lett. **59**, 52 (1987); Phys. Fluids **31**, 2714 (1988); P. Gibbon and A. R. Bell, Phys. Rev. Lett. **68**, 1535 (1992); M. K. Grimes *et al.*, *ibid.* **82**, 4010 (1999).

[16] L. M. Chen *et al.*, Phys. Rev. Lett. **87**, 225001 (2001); Y. T. Li *et al.*, Phys. Rev. E **64**, 046407 (2001); R. Kodama *et al.*, Phys. Plasmas **8**, 2268 (2001).

[17] Y. Toyama, Ph.D. thesis, Institute of Laser Engineering, Osaka University, Japan, 2003; Y. Toyama *et al.* (unpublished).

[18] S. C. Wilks, Phys. Fluids B **5**, 2603 (1993).

[19] F. N. Beg *et al.*, Phys. Plasmas **4**, 447 (1997).